Geophys. J. Int. (1997) **129**, 163–168

Curie-temperature depth estimation using a self-similar magnetization model

Stefan Maus, Dan Gordon and Derek Fairhead

Department of Earth Sciences, University of Leeds, Leeds LS2 9JT, *UK. E-mail: S.Maus@earth.leeds.ac.uk*

Accepted 1996 December 16. Received 1996 December 9; in original form 1996 September 14

SUMMARY

The Earth's crust is magnetized down to the Curie-temperature depth at about 10 to 50 km. This limited depth extent of the crustal magnetization is discernible in the power spectra of magnetic maps of South Africa and Central Asia. At short wavelengths, the power increases as rapidly towards longer wavelengths as expected for a self-similar magnetized crust with unlimited depth extent. Above wavelengths of about 100 km the power starts increasing less rapidly, indicating the absence of deep-seated sources. To quantify this effect we derive the theoretical power spectrum due to a slab carved out of a self-similar magnetization distribution. This model power spectrum matches the power spectra of South Africa and Central Asia for a self-similarity parameter of $\beta = 4$ and Curie temperature depths of 15 to 20 km.

Key words: fractals, geomagnetic field, magnetic anomalies.

INTRODUCTION

Ferrimagnetic minerals become paramagnetic (i.e. essentially non-magnetic) above their individual Curie temperature. Low-titanium titanomagnetite is likely to be the dominant source of the magnetic field in the lower continental crust (Schlinger 1985; Frost & Shive 1986). This mineral has Curie temperatures of 575°–600 °C (Schlinger 1985; Frost & Shive 1986; Wasilewski & Mayhew 1992), which corresponds to depths in the range of 10–50 km. Beneath this Curie-temperature depth the lithosphere is virtually non-magnetic. Furthermore, there is considerable petrological evidence from xenoliths that the Moho is also a magnetic boundary (Wasilewski, Thomas & Mayhew 1979; Mayhew, Johnson & Wasilewski 1985). While total magnetization levels can reach up to 100 A m^{-1} in mafic lower-crustal xenoliths, unaltered upper-mantle ultramafics have low magnetizations (Wasilewski & Mayhew 1992). In the following we will therefore use the more general term depth to bottom (DTB), leaving open whether the bottom is in fact a petrological or a temperature boundary.

Owing to the limited depth extent of the crustal magnetization, magnetic anomalies at the Earth's surface are damped at long wavelengths. The lack of long-wavelength power has been quantified in numerous studies to derive the DTB from magnetic surveys (Vacquier & Affleck 1941; Bhattacharyya & Leu 1975; Shuey *et al.* 1977; Connard, Couch & Gemperle 1983; Negi, Agrawal & Rao 1983; Blakely 1988; Herzfeld & Brodscholl 1994; Okubo *et al.* 1985; Okubo & Matsunaga 1994). Most of these investigations were based on the explicit or implicit assumption that long-wavelength anomalies necessarily originate only from deep-seated sources. If this were really the case, the limited depth extent of the crustal magnetization would already be visible in magnetic maps covering less than 100 km × 100 km. Indeed, Okubo *et al.* (1985) derived a detailed Curie isotherm map of the Island of Kyushu using 60 km × 90 km windows. Blakely (1995) recommends a minimum survey dimension of 50 km and 160 km for a DTB of up to 10 km and up to 50 km, respectively. On the other hand, Serson & Hannaford (1957) analysed aeromagnetic profiles extending over several thousand kilometres and failed to see the DTB because the auto-correlation did not taper off to zero, even for lags of several hundred kilometres.

Any method of DTB estimation requires a model for the magnetization distribution in the crust. Earlier models often failed to account for shallow long-wavelength variations in the magnetization. These variations are caused by regional geological features, such as extensive sedimentary basins, or contrasts between continental and oceanic lithosphere. One can argue that, on average, magnetization contrasts at long scales are similar to the ones observed at small scales. This idea leads to the powerful concept of self-similarity (Kolmogorov 1941; Mandelbrot 1983), which is consistent with susceptibility logs (Pilkington & Todoeschuck 1993; Maus & Dimri 1995), susceptibility surveys (Pilkington & Todoeschuck 1995) and magnetic maps (Gregotski, Jensen & Arkani-Hamed 1991; Pilkington & Todoeschuck 1993; Maus & Dimri 1995, 1996).

Here we derive a spectral density model for the anomaly of the total intensity of the magnetic field. The model accounts for the self-similarity as well as the limited depth extent of the crustal magnetization. We apply this model to investigate the

expected difference in the spectral density of magnetic maps for different DTBs.

MODEL

The potential of the magnetic field in a horizontal observation plane at a height z above a slab with thickness t of magnetic sources has been given by Naidu (1968, eq. 43, with $d_1 = z$ and $d_2 = z + t$):

$$\psi(x, y, z) = \frac{\mu_0}{2} \int_{-\infty}^{\infty}\int_{-\infty}^{\infty}\int_{-\infty}^{\infty} \tilde{\mathbf{J}}(u, v, w)\cdot(u\mathbf{e}_x + v\mathbf{e}_y + is\mathbf{e}_z) \times \frac{\exp(-sz)[\exp(-st - iwt) - 1]}{is(s + iw)} \times \exp(iux + ivy)\, dudvdw, \quad (1)$$

where $\tilde{\mathbf{J}}(u, v, w)$ is a spectral representation (e.g. Fourier transform) of the vector magnetization, $\mathbf{e}_x$, $\mathbf{e}_y$ and $\mathbf{e}_z$ are the unit vectors of the coordinate system, $\mathbf{s} = (u, v)^{\mathrm{T}}$ is the horizontal wavevector and $s = |\mathbf{s}|$.

Assuming that any remanent magnetization is either parallel or antiparallel to the geomagnetic field $\mathbf{N} = (n_x, n_y, n_z)^{\mathrm{T}}$, we can describe the magnetization by a virtual scalar susceptibility function $\chi(x, y, z)$ as $\mathbf{J}(x, y, z) = \chi(x, y, z)\mathbf{N}$. Owing to the linearity of the spectral representation, $\tilde{\mathbf{J}}(u, v, w) = \tilde{\chi}(u, v, w)\mathbf{N}$, and

$$\psi(x, y, z) = \frac{\mu_0}{2} \int_{-\infty}^{\infty}\int_{-\infty}^{\infty}\int_{-\infty}^{\infty} (un_x + vn_y + isn_z)\tilde{\chi}(u, v, w) \times \frac{\exp(-sz)[\exp(-st - iwt) - 1]}{is(s + iw)} \times \exp(iux + ivy)\, dudvdw. \quad (2)$$

Considering the anomaly of the total intensity of the magnetic field $T_a(x, y, z)$, which is related to the potential by $T_a = \mathbf{N}/|N| \cdot \nabla\psi$, gives

$$T_a(x, y, z) = \frac{\mu_0}{2|N|} \int_{-\infty}^{\infty}\int_{-\infty}^{\infty}\int_{-\infty}^{\infty} i(un_x + vn_y + isn_z)^2 \tilde{\chi}(u, v, w) \times \frac{\exp(-sz)[\exp(-st - iwt) - 1]}{is(s + iw)} \times \exp(iux + ivy)\, dudvdw. \quad (3)$$

Then a 2-D spectral representation of the magnetic field is given by

$$\tilde{T}_a(u, v, z) = \frac{\mu_0}{2|N|} i(un_x + vn_y + isn_z)^2 \exp(-sz) \times \int_{-\infty}^{\infty} \tilde{\chi}(u, v, w) \frac{[\exp(-st - iwt) - 1]}{is(s + iw)}\, dw. \quad (4)$$

Let us denote the horizontal component of the geomagnetic field by H and the angle between the horizontal projection $\mathbf{H}$ of the field and the horizontal wavevector $\mathbf{s}$ by θ. Then

$$\tilde{T}_a(u, v, z) = \frac{\mu_0}{2|N|} (n_z + iH\cos\theta)^2 s \exp(-sz) \times \int_{-\infty}^{\infty} \tilde{\chi}(u, v, w) \frac{[1 - \exp(-st - iwt)]}{(s + iw)}\, dw. \quad (5)$$

The spectral representation $\tilde{T}_a(u, v, z)$ of the magnetic field can be regarded as a convolution of the spectral representation $\tilde{\chi}(u, v, w)$ of the susceptibility distribution with a function $\varphi(w)$:

$$\tilde{T}_a(u, v, z) = \int_{-\infty}^{\infty} \varphi(w)\tilde{\chi}(u, v, w)\, dw, \quad (6)$$

where

$$\varphi(w) = \frac{\mu_0}{2|N|} (n_z + iH\cos\theta)^2 s \exp(-sz) \frac{[1 - \exp(-st - iwt)]}{(s + iw)}. \quad (7)$$

Up to this point one could think of the spectral representations as Fourier transforms on the basis of the usual Riemann integral. Taking this view, $\tilde{T}_a(u, v, z)$ and $\tilde{\chi}(u, v, w)$ are deterministic functions, obtained by an integral transform from the space-domain magnetic field $T_a(x, y, z)$ and the space-domain susceptibility distribution $\chi(x, y, z)$. In the following, we shall take a stochastic point of view. Then $T_a(x, y, z)$ and $\chi(x, y, z)$ are regarded as the outcome of some kind of random experiment. Their spectral representations are given by Fourier–Stieltjes integrals (Yaglom 1986) in the following sense:

$$R(x) = \int_{-\infty}^{\infty} \exp(iux) Z(du), \quad (8)$$

where $R(x)$ is the random function in the space domain and $Z(du)$ is a complex random measure determined for any interval du and having the properties

(1) $\langle Z(du)\rangle = 0$ for all intervals du;
(2) $\langle Z(du)\overline{Z(du')}\rangle = 0$ for non-intersecting intervals du and du';
(3) $Z(du \cup du') = Z(du) + Z(du')$ for non-intersecting intervals du and du'.

The spectral density $f(u)$, if it exists, is related to $Z(du)$ by

$$\langle Z(du)\overline{Z(du)}\rangle = f(u)\, du. \quad (9)$$

Finally,

$$\langle Z(du)\overline{Z(du')}\rangle = \delta(u - u') f(u)\, dudu'. \quad (10)$$

Here, $\langle . \rangle$ stands for the expected value and $\delta(u)$ is the Dirac delta-function.

In this notation, eq. (6) becomes

$$\tilde{T}_a(du, dv, z) = \int_{-\infty}^{\infty} \varphi(w)\tilde{\chi}(du, dv, dw), \quad (11)$$

where $\tilde{T}_a(du, dv, z)$ and $\tilde{\chi}(du, dv, dw)$ are two random measures, corresponding to $Z(du)$ in eq. (8). An application of the Fourier–Stieltjes integral to a related problem can be found in Maus & Dimri (1996). To derive an expression for the spectral density of the magnetic field, we multiply both sides of (11) with their complex conjugates and make use of the properties (9) and (10):

$$\tilde{T}_a(du, dv, z)\overline{\tilde{T}_a(du, dv, z)} = \int_{-\infty}^{\infty}\int_{-\infty}^{\infty} \varphi(w)\tilde{\chi}(du, dv, dw)\overline{\varphi(w')\tilde{\chi}(du, dv, dw')}, \quad (12)$$

$$f_T(u, v, z)\,du dv = \int_{-\infty}^{\infty}\int_{-\infty}^{\infty} \varphi(w)\overline{\varphi(w')}\delta(w-w') f_\chi(u, v, w)\,du dv dw dw', \quad (13)$$

$$f_T(u, v, z) = \int_{-\infty}^{\infty} \varphi(w)\overline{\varphi(w)} f_\chi(u, v, w)\,dw, \quad (14)$$

where $f_T(u, v, z)$ is the spectral density of the magnetic field and $f_\chi(u, v, w)$ is the spectral density of the susceptibility distribution within the slab. Recalling the definition of $\varphi(w)$ from eq. (7),

$$\varphi(w)\overline{\varphi(w)} = \frac{\mu_0^2}{4N^2}(n_z + iH\cos\theta)^2\overline{(n_z + iH\cos\theta)^2}s^2\exp(-2sz) \times \frac{1-\exp(-st-iwt)}{s+iw}\overline{\left(\frac{1-\exp(-st-iw't)}{s+iw'}\right)} \quad (15)$$

$$= \frac{\mu_0^2}{4N^2}(n_z^2 + H^2\cos^2\theta)^2 s^2\exp(-2sz) \times [1-\exp(-ts-itw)-\exp(-ts+itw) + \exp(-2ts)](s^2+w^2)^{-1} \quad (16)$$

$$= \frac{\mu_0^2}{4N^2}(n_z^2 + H^2\cos^2\theta)^2 s^2\exp(-2sz) \times 2\exp(-ts)[\cosh(ts)-\cos(tw)](s^2+w^2)^{-1}. \quad (17)$$

Combining eqs (14) and (17) leads to a relationship between the spectral density of the magnetic field and the spectral density of the susceptibility distribution within the slab:

$$f_T(u, v, z) = \frac{\mu_0^2}{2N^2}(n_z^2 + H^2\cos^2\theta)^2\exp(-2sz-ts) \times \int_{-\infty}^{\infty}[\cosh(ts)-\cos(tw)]\left(1+\frac{w^2}{s^2}\right)^{-1} \times f_\chi(u, v, w)\,dw. \quad (18)$$

Assuming self-similarity of $\chi(x, y, z)$ is expressed by

$$f_\chi(u, v, w) = c_s(u^2+v^2+w^2)^{-\beta/2} \quad (19)$$

$$= c_s s^{-\beta}\left(1+\frac{w^2}{s^2}\right)^{-\beta/2}, \quad (20)$$

where c_s and β are constants, β being the 3-D scaling exponent of the susceptibility distribution. Substitution of eq. (20) into eq. (18) gives the 2-D spectral density (power spectrum) of the magnetic field due to a slab of self-similar sources:

$$f_T(u, v, z) = c_s\frac{\mu_0^2}{N^2}(n_z^2 + H^2\cos^2\theta)^2\exp(-2sz-ts)s^{-\beta} \times \int_0^{\infty}[\cosh(ts)-\cos(tw)]\left(1+\frac{w^2}{s^2}\right)^{-1-\beta/2} dw. \quad (21)$$

It is common practice to work with the logarithm of the radially averaged power spectrum (Spector & Grant 1970). However, instead of the logarithm of the radial average power, it is advisable to take the radial average of the logarithm of the power (Maus & Dimri 1995), as in

$$\frac{1}{2\pi}\int_0^{2\pi}\ln(f_T)\,d\theta = \underbrace{\frac{1}{2\pi}\int_0^{2\pi}\ln\left[c_s\frac{\mu_0^2}{N^2}(n_z^2+H^2\cos^2\theta)^2\right]d\theta}_{C} - 2sz - ts - \beta\ln(s) + \ln\left[\int_0^{\infty}[\cosh(ts)-\cos(tw)]\left(1+\frac{w^2}{s^2}\right)^{-1-\beta/2} dw\right]. \quad (22)$$

The anisotropy of the field is then reflected only in the term C, which is independent of the wavenumber s. Consequently, it is not necessary to reduce the spectrum to the pole. This is particularly welcome at low magnetic latitudes, where a reduction to the pole is difficult because $(n_z^2 + H^2\cos^2\theta)^2$ becomes small for $\theta = 90°$.

Limitations of the theory

Eq. (1) is based on the implicit assumption that the magnetic field as well as its source distribution can be written as a Fourier integral. This contradicts the self-similarity assumption in eq. (20). A self-similar random function cannot be represented as a sum of harmonic waves. The same objection applies to *white noise*, which is often used as a model for source distributions. In this case the problem of a diverging Fourier integral is avoided by assuming *band-limited white noise*. In the same way one can assume that the self-similarity of a stochastic process is restricted to a limited band of wavenumbers (Goff & Jordan 1988; Maus & Dimri 1996). Nevertheless, eqs (21) and (22) have to be regarded as approximations rather than exact relations. The quality of the approximation is likely to vary with the value of β.

RESULTS

Using eq. (22), we investigate the possibilities and limitations of DTB estimation from the power spectrum of total-field magnetic-anomaly maps. The model power spectra are obtained by numerical evaluation of (22) for a particular set of model parameters. These model power spectra are then plotted against power spectra of different survey areas. The constant C in eq. (22) is chosen in such a way that the model power spectrum fits the power spectrum of the magnetic map at high wavenumbers.

Survey areas

Our first sample power spectrum is taken from the literature. It was estimated in the usual way by Whaler (1994) from aeromagnetic and Magsat data of South Africa downward-continued to surface level. This power spectrum is displayed together with the model power spectra of eq. (22) for $z = 0$ and various scaling exponents and slab thicknesses in Figs 1–3.

Since eq. (22) is actually a model for the radial average of the log power and not for the log of the radially averaged power, we have estimated our own power spectra from two large magnetic grids of the former Soviet Union (FSU),

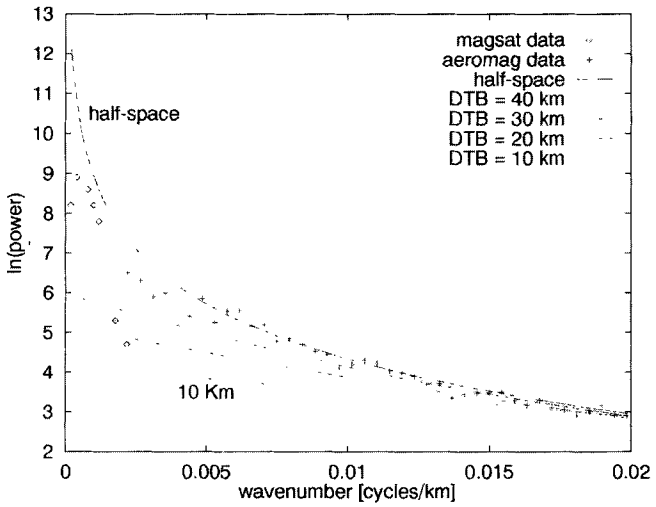

Figure 1. Power spectra of aeromagnetic and Magsat grids over South Africa (after Whaler 1994, Fig. 10), together with the model power spectra of eq. (22) for $\beta = 3$, $z = 0$ and various DTBs. The half-space model corresponds to an infinite DTB.

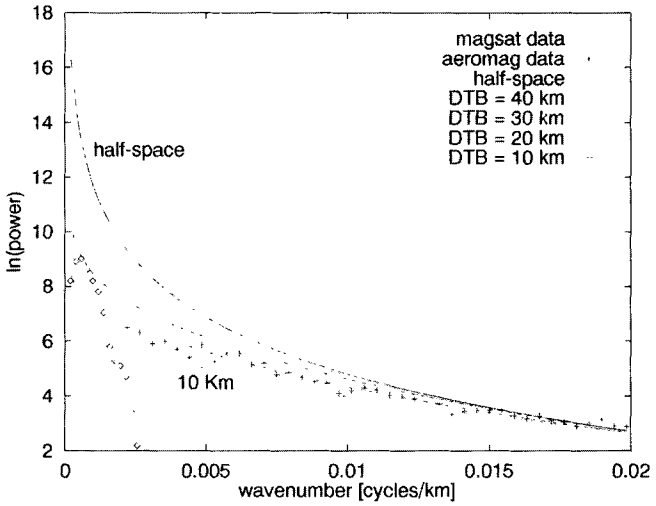

Figure 2. Data of Fig. 1 together with the model power spectra for $\beta = 4$.

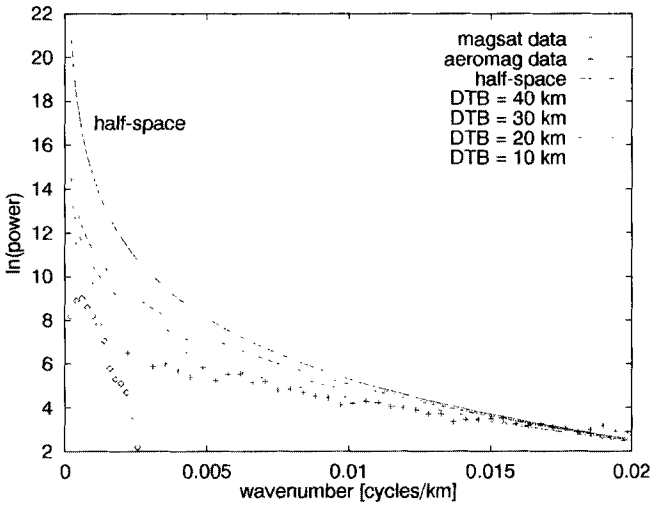

Figure 3. Data of Fig. 1 together with the model power spectra for $\beta = 5$.

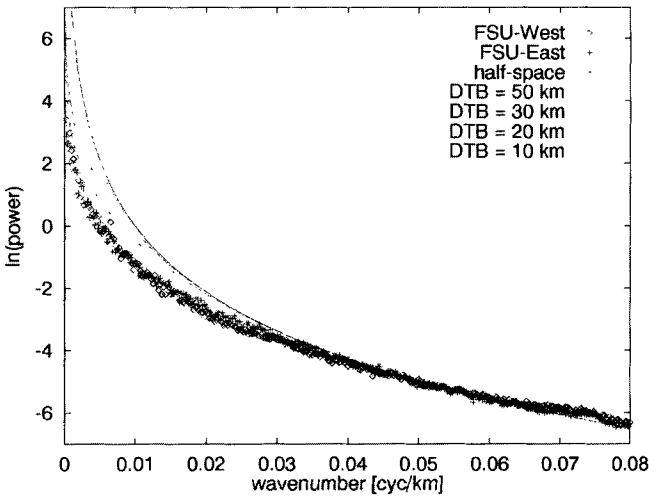

Figure 4. Power spectra of the former Soviet Union together with the model power spectra for $\beta = 4$ and $z = 300$ m. The power spectra of the magnetic maps are scaled in such a way that the integral over the 2-D power spectrum is equal to the expected value for $|T_a|^2$ in nanoteslas.

available from the National Geophysical Data Center, Boulder, Colorado. The grids were compiled from surveys flown at 200 to 500 m topographic altitude. The grid FSU-West extends from 35° to 78° latitude and 61° to 104° longitude, while the grid FSU-East has the same latitude but extends from 104° to 147° in longitude. The IGRF of 1965 and a first-order trend were removed from the data. Their power spectra are shown in Figs 4 to 7. The graphs in Figs 5 and 6 are plotted on a log–log scale to demonstrate the self-similarity of the magnetic field at high wavenumbers and the departure from self-similarity at low wavenumbers.

Resolution of the depth to bottom (DTB)

It is not our intention to derive precise DTB estimates of the survey areas, but to investigate the possibilities and limitations of DTB estimation in general. From the plots in Figs 1–6 we draw the following conclusions.

(1) A noticeable difference between the model power spectra for different DTBs occurs only at wavelengths above 100 km (see in particular Fig. 6).

(2) We find a trade-off between increasing susceptibility scaling exponents β and a decreasing DTB. A scaling exponent of $\beta = 4$ gives a realistic DTB of about 20 km for South Africa (Fig. 2). For Central Asia a scaling exponent of $\beta = 4$ leads to a DTB of 15 ± 5 km (Figs 4 and 5). This may be too shallow. Choosing a lower scaling exponent of $\beta = 3.5$ leads to a DTB estimate of almost 50 km (Fig. 6). Hence, the fact that the exact value of the scaling exponent β of the crustal susceptibility distribution is unknown leads to large uncertainties in absolute DTB estimates.

(3) To resolve the power at long wavelengths with sufficient precision, large survey areas are required. It is unlikely that a reliable estimate of the DTB can be obtained from an area smaller than 1000 km × 1000 km. Consequently, it could be difficult to estimate the DTB from individual aeromagnetic

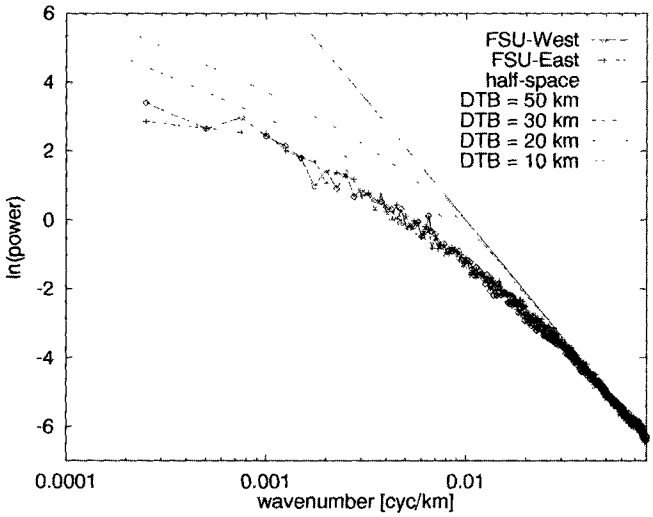

Figure 5. Data of Fig. 4 in log–log scale. At high wavenumbers the magnetic field is self-similar and its log–log power spectrum is a straight line. At wavelengths above 50 km (corresponding to wavenumbers below 0.02 cycles km^{-1}) the power is decreased due to the limited depth extent of the crustal magnetization. The model indicates a DTB of about 15 km under the assumption of $\beta = 4$.

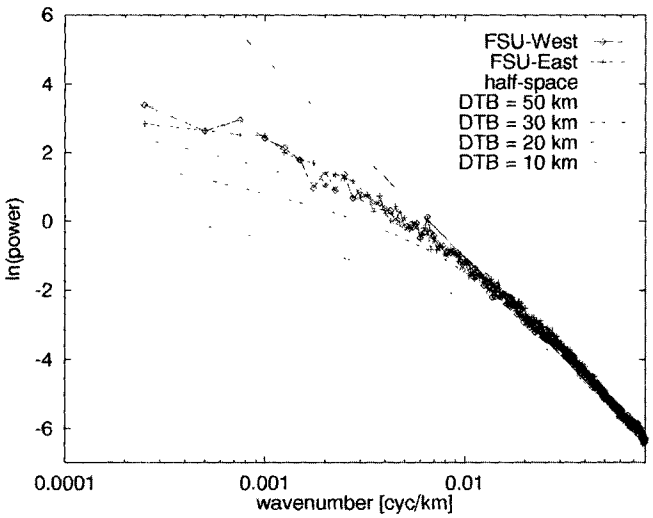

Figure 6. Power spectra of the FSU in log–log scale as in Fig. 5 but with the model power spectra for $\beta = 3.5$. The lower the assumed scaling exponent of the crustal susceptibility distribution, the greater the resulting estimate for the DTB.

surveys, typically having dimensions of not more than a few hundred kilometres. The situation may, however, be more favourable for young oceanic crust with shallower DTB.

(4) A consequence of the large survey areas required is that realistic maps of the DTB will have a very low lateral resolution. It is unlikely that it will be possible to resolve lateral DTB variations for distances of less than several hundred kilometres from magnetic data by spectral methods. Such DTB maps would not shed much light on geological features with strong lateral temperature variations, such as subduction zones.

One also has to take into consideration that long-wavelength anomalies in continental-scale magnetic compilations can be

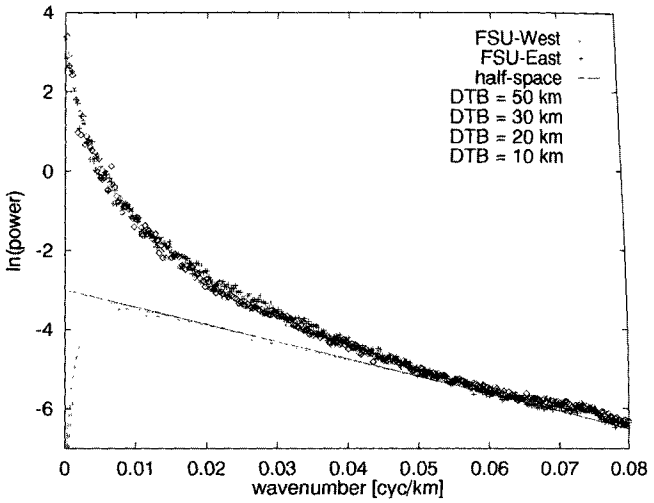

Figure 7. Power spectra of the FSU with the model power spectra for $\beta = 1$ and $z = 3.5$ km. This corresponds to an interpretation using the white depth models that were utilized in earlier studies to derive the DTB from the location of a maximum in the power spectrum. There is no maximum in the FSU power spectra. Maxima are only found in power spectra that are inaccurately derived from small survey areas.

severely compromised by survey stitching procedures, non-uniform data acquisition parameters (especially the elevation) and by the choice of geomagnetic reference field.

Long-range correlation

We infer from Figs 1–6 that a susceptibility scaling exponent of $\beta \approx 4$ is consistent with the magnetic maps of South Africa and Central Asia. This is an important result, because it implies that the scaling law observed by Pilkington & Todoeschuck (1993) and Pilkington, Todoeschuck & Gregotski (1994) for susceptibility logs and surveys on a local scale can also be valid at regional scales of up to thousands of kilometres. In particular, the crustal magnetization can be correlated over considerable distances. This contradicts earlier assumptions of correlation lengths only up to several tens of kilometres (Jackson 1990, 1994).

White depth models

To compare our results with those of earlier studies, let us attempt to interpret the FSU spectra in the conventional way (Spector & Grant 1970; Connard *et al.* 1983). The slope of the power spectrum thus indicates the depth to the top of some kind of statistical ensemble of prisms. The limited depth extent of these prisms leads to a maximum in the power spectrum (Spector & Grant 1970). The wavenumber of this maximum is directly related to the DTB (Blakely 1995). This interpretation is based on the implicit assumption of a white power spectrum of the magnetic field at source level. Hence, it corresponds to $\beta = 1$ in terms of our model. Fig. 7 shows the corresponding power spectra. The obvious disagreement with the observed power spectra, in particular the missing maxima, is a further indication that white depth models should not be used to estimate the depth to the bottom of a magnetic layer.

DISCUSSION

We have derived a spectral model for magnetic maps at a regional scale. Long-range correlation is accounted for by the scaling exponent of a virtual susceptibility distribution. The higher the value of β, the stronger the long-range correlation.

For $\beta = 1$ our model describes the field due to a weakly correlated crustal magnetization as assumed by the popular *white noise* field models (Hahn, Kind & Mishra 1976). Many earlier DTB estimates are based on such models. Fig. 1 shows, however, that realistic values of β are certainly above $\beta = 3$. Consequently, the DTB is manifested much less prominently in magnetic maps than assumed in earlier studies.

Nevertheless, it seems to be possible to compute maps of the DTB. The main obstacles are the low resolution and the trade-off between higher scaling exponents β and shallower DTBs. Resolution of the DTB requires an assumption about β. Values of β could be larger in the lower than in the upper crust, indicating a smoother distribution of magnetization. However, assuming a constant value of $\beta = 4$ and moving a window over a very large area would probably lead to a smooth DTB relief, with a certain degree of uncertainty in the absolute depth.

Perhaps our most interesting finding is that the self-similarity of the crustal magnetization extends with a high scaling exponent of $\beta_{3\text{-D}}$ close to 4 up to regional wavelengths. The 3-D scaling exponent $\beta_{3\text{-D}}$ of the susceptibility distribution is related to the scaling exponents of lower-dimensional cross-sections of the same distribution by $\beta_{3\text{-D}} = \beta_{2\text{-D}} + 1 = \beta_{1\text{-D}} + 2$ (Maus & Dimri 1994). A $\beta_{3\text{-D}}$ of close to 4 therefore agrees well with the results of earlier studies that suggest that the susceptibility distribution in the crust has scaling exponents of $\beta_{1\text{-D}} \approx 2$ (Pilkington & Todoeschuck 1993) and $\beta_{2\text{-D}} \approx 3$ (Pilkington & Todoeschuck 1995). Furthermore, the corresponding magnetic field at surface level should have a 2-D scaling exponent of $\gamma_{2\text{-D}} = \beta_{3\text{-D}} - 1$. Indeed, Gregotski *et al.* (1991) found scaling exponents of $\gamma_{2\text{-D}} \approx 3$ for local magnetic anomalies in North America. Significantly lower scaling exponents of $\beta_{1\text{-D}} = 0.4$ and $\gamma_{2\text{-D}} \approx 2$ were found for the susceptibility distribution and the magnetic field in the area of the German Continental Deep Drilling Project (Maus & Dimri 1995).

ACKNOWLEDGMENTS

This paper has benefited from discussions with Andy Jackson, Jeff Love, Vincent Lesur and Alan Reid, as well as from helpful comments of John Kent and two anonymous reviewers.

REFERENCES

Bhattacharyya, B.K. & Leu, L.K., 1975. Analysis of magnetic anomalies over Yellowstone National Park: mapping Curie point isothermal surface for geothermal reconnaissance, *J. geophys. Res.*, **80,** 4461–4465.

Blakely, R.J., 1988. Curie temperature isotherm analysis and tectonic implications of aeromagnetic data from Nevada, *J. geophys. Res.*, **93,** 11 817–11 832.

Blakely, R.J., 1995. *Potential Theory in Gravity and Magnetic Applications,* Cambridge University Press, Cambridge.

Connard, G., Couch, R. & Gemperle, M., 1983. Analysis of aeromagnetic measurements from the Cascade Range in central Oregon, *Geophysics,* **48,** 376–390.

Frost, B.R. & Shive, P.N., 1986. Magnetic mineralogy of the lower continental crust, *J. geophys. Res.*, **91,** 6513–6521.

Goff, J.A. & Jordan, T.H., 1988. Stochastic modeling of seafloor morphology: Inversion of sea beam data for second-order statistics, *J. geophys. Res.*, **93,** 13 589–13 608.

Gregotski, M.E., Jensen, O. & Arkani-Hamed, J., 1991. Fractal stochastic modeling of aeromagnetic data, *Geophysics,* **56,** 1706–1715.

Hahn, A., Kind, E.G. & Mishra, D.C., 1976. Depth estimation of magnetic sources by means of Fourier amplitude spectra, *Geophys. Prospect.*, **24,** 287–308.

Herzfeld, U.C. & Brodscholl, A.L., 1994. On the geologic structure of the Explora Escarpment (Weddell Sea, Antarctica) revealed by satellite and shipboard data evaluation, *Marine geophys. Res.*, **16,** 325–345.

Jackson, A., 1990. Statistical treatment of crustal magnetization, *Geophys. J. Int.*, **119,** 991–998.

Jackson, A., 1994. Accounting for crustal magnetization in models of the core magnetic field, *Geophys. J. Int.*, **103,** 657–673.

Kolmogorov, A.N., 1941. Local structure of turbulence in an incompressible fluid at very high Reynolds numbers, *Dokl. Akad. Nauk SSSR,* **30,** (4), 299–303.

Mandelbrot, B.B., 1983. *The Fractal Geometry of Nature,* W.H. Freeman, New York, NY.

Maus, S. & Dimri, V.P., 1994. Scaling properties of potential fields due to scaling sources, *Geophys. Res. Lett.*, **21,** 891–894.

Maus, S. & Dimri, V.P., 1995. Potential field power spectrum inversion for scaling geology, *J. geophys. Res.*, **100,** 12 605–12 616.

Maus, S. & Dimri, V.P., 1996. Depth estimation from the scaling power spectrum of potential fields, *Geophys. J. Int.*, **124,** 113–120.

Mayhew, M., Johnson, B.D. & Wasilewski, P., 1985. A review of problems and progress in studies of satellite magnetic anomalies, *J. geophys. Res.*, **90,** 2511–2522.

Naidu, P., 1968. Spectrum of the potential field due to randomly distributed sources, *Geophysics,* **33,** 337–345.

Negi, J.G., Agrawal, P.K. & Rao, K.N.N., 1983. Three-dimensional model of the Koyna area of Maharashtra State (India) based on the spectral analysis of aeromagnetic data, *Geophysics,* **48,** 964–974.

Okubo, Y. & Matsunaga, T., 1994. Curie point depth in northeast Japan and its correlation with regional thermal structure and seismicity, *J. geophys. Res.*, **99,** 22 363–22 371.

Okubo, Y., Graf, R.J., Hansen, R.O., Ogawa, K. & Tsu, H., 1985. Curie point depths of the island of Kyushu and surrounding areas, Japan, *Geophysics,* **50,** 481–494.

Pilkington, M. & Todoeschuck, J.P., 1993. Fractal magnetization of continental crust, *Geophys. Res. Lett.*, **20,** 627–630.

Pilkington, M. & Todoeschuck, J.P., 1995. Scaling nature of crustal susceptibilities, *Geophys. Res. Lett.*, **22,** 779–782.

Pilkington, M., Todoeschuck, J.P. & Gregotski, M.E., 1994. Using fractal crustal magnetization models in magnetic interpretation, *Geophys. Prospect.*, **42,** 677–692.

Schlinger, C.M., 1985. Magnetization of lower crust and interpretation of regional crustal anomalies: Example from Lofoten and Vesterøalen, Norway, *J. geophys. Res.*, **90,** 11 484–11 504.

Serson, P.H. & Hannaford, W., 1957. A statistical analysis of magnetic profiles, *J. geophys. Res.*, **62,** 1–18.

Shuey, R.T., Schellinger, D.K., Tripp, A.C. & Alley, L.B., 1977. Curie depth determination from aeromagnetic spectra, *Geophys. J. R. astr. Soc.*, **50,** 75–101.

Spector, A. & Grant, F.S., 1970. Statistical models for interpreting aeromagnetic data, *Geophysics,* **35,** 293–302.

Vacquier, V. & Affleck, J., 1941. A computation of the average depth to the bottom of the Earth's magnetic crust, based on a statistical study of local magnetic anomalies, *Trans. Am. geophys. Un.,* **22,** 446–450.

Wasilewski, P. & Mayhew, M., 1992. The Moho as a magnetic boundary revisited, *Geophys. Res. Lett.*, **19,** 2259–2262.

Wasilewski, P., Thomas, H. & Mayhew, M., 1979. The Moho as a magnetic boundary, *Geophys. Res. Lett.*, **6,** 541–544.

Whaler, K.A., 1994. Downward continuation of Magsat lithospheric anomalies to the Earth's surface, *Geophys. J. Int.*, **116,** 267–278.

Yaglom, A.M., 1986. Correlation Theory of Stationary and Related Random Functions, Vol. 1, Springer-Verlag, New York, NY.